Driver's Intention Identification and Risk Evaluation at Intersections in the Internet of Vehicles

Chen Chen, *Member, IEEE*, Lei Liu, Tie Qiu, *Senior Member, IEEE*, Zhiyuan Ren, *Member, IEEE*, Jinna Hu, and Fang Ti

***Abstract*—In recent years, the rapid improvement of sensor and wireless communication technologies powerfully impels the development of advanced cooperative driving systems, generating the demands to form the Internet of Vehicles (IoV). With the assistance of cooperative communication among vehicles, the road safety can be greatly enhanced in the IoV. In this paper, we propose a cooperative driving scheme for vehicles at intersections in the IoV. First, the driver's intention is modeled by the BP neural network trained with driving dataset. Then, the identified intention is used as the control matrix of the Kalman filter model, by which the vehicle trajectory can be predicted. Finally, by collecting the information of vehicles' trajectories at the intersections, we develop a collision probability evaluation model to reflect the conflict level among vehicles at intersections. Through obtained collision probability, the driver or the autonomous control unit can determine the next step to avoid the possible collisions. Numerical results show that our proposed scheme has high accuracy in terms of driver's intention identification, trajectory prediction and collision probability evaluation.**

***Index Terms*—Internet of vehicles (IoV), intersection, neural network, safety risk assessment.**

I. Introduction

In recent years, with the rapid development of automobile industry, the car ownership has been dramatically increased. This leads to a series of traffic issues, especially a surge in traffic accidents, seriously affecting the safety of people's life and property. Under this situation, the intelligent transportation systems (ITSs) have attracted more and more attentions for their potential in improving traffic efficiency and guaranteeing traffic safety [1].

Manuscript received September 16, 2017; revised December 11, 2017; accepted December 22, 2017. Date of publication January 1, 2018; date of current version June 8, 2018. This work was supported in part by the National Natural Science Foundation of China under Grant 61571338, Grant U1709218, and Grant 61672131, in part by the Key Research and Development Plan of Shaanxi Province under Grant 2017ZDCXL-GY-05-01, in part by the Open Fund of the State Key Laboratory of Integrated Services Networks under Grant ISN16-03, in part by the National Key Research and Development Program of China under Grant 2016YFE0123000, in part by the National Science and Technology Major Project of the Ministry of Science and Technology of China under Grant 2015zx03002006-003, and Grant MJ-2014-S-37, and in part by the 111 Project of China under Grant B08038. *(Corresponding author: Tie Qiu.)*

C. Chen, L. Liu, Z. Ren, J. Hu, and F. Ti are with the State Key Laboratory of Integrated Service Networks, Xidian University, Xi'an 710071, China (e-mail: cc2000@mail.xidian.edu.cn; tianjiaoliulei@163.com; zyren@xidian.edu.cn; 476060689@qq.com).

T. Qiu is with the School of Computer Science and Technology, Tianjin University, Tianjin 300350, China (e-mail: qiutie@ieee.org).

Digital Object Identifier 10.1109/JIOT.2017.2788848

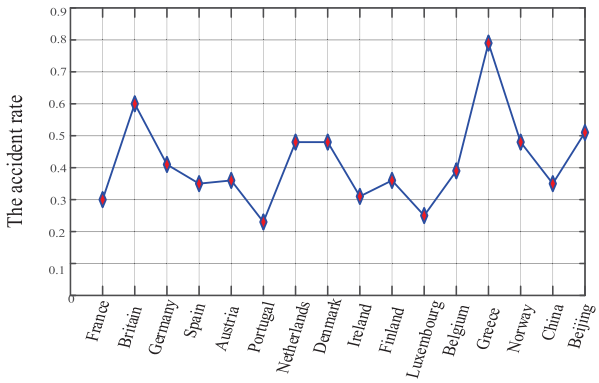

Fig. 1. Traffic accident rate at intersections in different countries.

On the other hand, as the transportation hub, the intersection is an important element of road traffic systems. The presence of intersections enables the high level of the transportation flexibility and accessibility, enhancing the activity as well as perfecting the function of the road network. At the same time, however, being the throat of city traffic, without reasonable and effective management, intersections also easily become road bottlenecks. For example, at intersections, traffic accidents can frequently occur due to serious interferences from vehicles and pedestrians, vehicles and vehicles (especially motor vehicles and nonmotor vehicles). The statistical results have revealed that among all the traffic accidents, the ones that occur at intersections account for a large proportion. Fig. 1 shows that the accident rate at intersections in different countries. From this figure, it can be found that in China, the number of traffic accidents at intersections is about 30% of the total number of accidents, which indicates the importance of intersections for the driving safety of the entire urban road system. Therefore, it is very necessary to present an analytical model for accident probability at intersections to predict the general pattern and trend of the occurrence of accidents, with the aim to provide the guidance for improving the urban road traffic safety.

To reach above goal, as one important component of ITSs, the Internet of vehicles (IoV) composed of vehicles and road infrastructures can be a better candidate, which can alleviate the road congestion, increasing the road capacity, improving the traffic managing efficiency as well as enhancing the road safety [2]. For example, the safety related applications, such as cooperative collision avoidance [3], violation of traffic signal

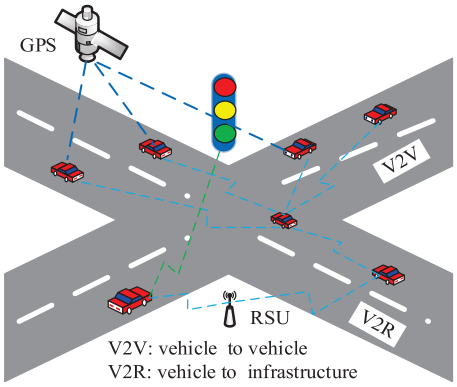

Fig. 2. Discussed intersection case.

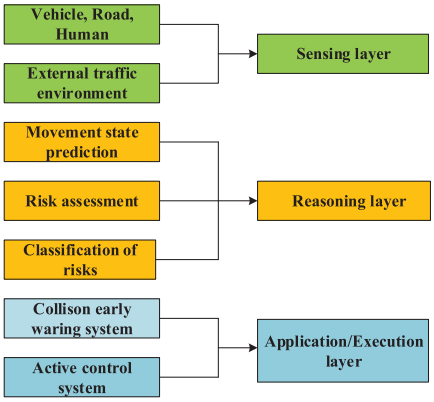

Fig. 3. General structure of cooperative driving systems.

violation warning [4], lane change warning [5], can be realized with the help of IoV to significantly improve the driving safety between vehicles to vehicles and vehicles to pedestrians.

Fig. 2 shows a typical scenario of IoV at intersections, where the vehicle could avoid collisions to each other or from pedestrians by action in advance upon the receiving of early warnings or even autonomous control instructions. These early warnings and autonomous controls can be issued by the on-board units of cars own or neighboring cars, or road side units along the roadside, through the awareness among different vehicles with the help of advanced localization [global positioning system (GPS)] and communication technologies. In this paper, we also propose a cooperative driving scheme relying on early warning or autonomous controls of vehicles at intersections, based on driver's intention identification and driving risk evaluation in the IoV.

Generally speaking, as shown in Fig. 3, a cooperative driving system is composed of following elements: the sensing layer, the reasoning layer (or inferencing layer), and the application layer (or execution layer). The sensing layer is responsible of collecting the environment information to improve awareness of vehicles, referring to road, driver, status of vehicles own and neighboring vehicles, etc., by wireless communication and sensor measurement. The sensing layer then sends the collected information to the reasoning layer. After that, the reasoning layer determines each vehicle' state and corresponding risk level using the information from the sensing layer. Finally, the application (or execution layer) could adjust the vehicular dynamics according to the evaluated risks to avoid the potential occurrence of traffic accidents as well as warn the other vehicles as early as possible. By now, the researches on the design of cooperative driving systems have actually attracted much attentions from industrial and academic communities. Aswad *et al.* [6] designed an environment-aware auxiliary driving system. The system first obtains the information of vehicles and their surroundings, and then finds one appropriate vehicle state pattern matching the collected information from the pattern library. Finally, it uses the identified vehicle state pattern to guide the drivers on how to drive. Woerndl *et al.* [7] presented an information-aware architecture in ITSs, which is further divided into three parts, namely the physical perception part, the reasoning decision part, and the vehicle execution part. The physical perception will pass the collected information by sensors to the reasoning decision layer. Based on the collected information, the reasoning decision layer uses the dynamic Bayesian network to predicate the vehicle movement state, and then send these results to the vehicle execution part. Upon receiving these results, the vehicle execution part performs the corresponding actions, involving early warnings and autonomous control, to guarantee the driving safety.

In summary, although there have been already many works proposed in cooperative driving system design, the existing safety enhancement systems often lead to an inaccurate estimation to the potential road risks. The reason has twofolds. The first factor lies on the ignoring of the prodigious disjunction between the actual intentions of drivers and actual warning or control/actions of vehicles, by which an erroneous driving operation may be issued resulting in accidents. Therefore, a precise estimation to the real intentions of drivers especial for neighboring cars, is of great importance to ensure the following issued warnings or controls are convincible. The second factor focuses on the risk evolution during driving, where an overestimated or underestimated risk is often suggested without fully considerations on the practical trajectories of vehicles and real intentions of drivers on the investigated and neighboring cars.

As a result, in this paper, we focus on the design of the reasoning layer as shown in Fig. 3 and predict the collision probability with the inference of drivers' intensions and trajectories of vehicles. Based on drivers' intentions, we propose a method to calculate the collision probability of vehicles at intersections by estimating the conflict between vehicles' trajectories. The simplified flowchart of our scheme is depicted as shown in Fig. 4. At first, we make use of the BP neural network to build the driver's intention-inference model with training dataset. Then, the identified intention is used as the control matrix of the Kalman filter model, on the basis of which the vehicle trajectory can be predicted. Finally, according to the prediction trajectory, we can obtain the collision probability of vehicles at intersections. Thus, according to the evaluated collision probability, the driver or autonomous control unit can determine whether some measures should be taken in advance to avoid the possible collisions.

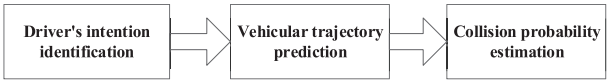

Fig. 4. Simplified flowchart of our scheme.

The main contributions of this paper are generalized as follows.

1) Considering that the driver's behavior is time-varying in the complex traffic environment, it is difficult to identify the intentions of drivers across a time span. To deal with this issue, we establish a driver's intention inference model with the help of the trained BP neural network.
2) In order to provide the guidance for the collision evaluation module, we use the Kalman filter model to predict the trajectories of vehicles and their real-time movement status, for collision conflict determination.
3) In order to make one accurate evaluation risk, we establish a novel collision probability model based on vehicles' travel trajectories.

The remainder of this paper is organized as follows. Section II provides a review of existing related works. The framework of our proposed model is presented in Section III. The driver's intention identification model is demonstrated in Section IV. In Section V, the mechanism used to predict the vehicular trajectory is introduced. Section VI presents the collision probability estimation module in detail. The performance of our proposal is evaluated in Section VII. Finally, this paper is concluded in Section VIII.

II. Related Work

Be reviewing previous studies in cooperative driving technologies, it can be found that this research filed is actually much mature and mainly consists of three components or steps, i.e., driver's intention identification, vehicular position or trajectory prediction and collision probability estimation, corresponding to the flowchart in Fig. 4. Next, we generalize some typical works with respect to above three components.

A. Driver's Intention Identification

In general, the driver produced the intention with the objective of guiding the subsequent behavior to make the vehicle drive in accordance with the wish of the driver. The study in [8] suggested that people's faulty decision or even behavior during driving is an important reason of road traffic accidents. Actually, due to the driver's erroneous driving operation, the vehicle is malfunctioning, leading to the occurrence of traffic accidents. However, the driver's actual or original intention is that the accident should not be caused by the vehicle's out-of-control. Instead, she/he hopes that the operation can make the vehicle get out of the out-of-control state. That indicates there is a prodigious disjunction between the actual intention of drivers and actual control/action of vehicles. Therefore, it is much necessary to design one intention speculate mechanism to accurately identify driver's intention as early as possible. Husen and Lee [9] proposed a method to analyze drivers' behaviors based on syntactic recognition, and used the context-free grammar to change drivers' behaviors. In their paper, the grammar is trained with driving data including the driver's attention time, speed of the car and angle of the steering wheel. The generated signal indication, which is expressed in symbolic form, forms a sentence representing the specific behavior. After that, their model then evaluates the syntax by parsing the formed sentences to detect the driving behavior. Although their scheme is practical and effective for driving safety enhancement, the detection and recognition rate of their system still need further improvement. He *et al.* [10] proposed a double hidden Markov model to identify driving intent and then predict following driving behavior of the driver. In their model, the driving behaviors are recognized by manoeuvring the signals of the driver and vehicle state information. Numerical results showed that their model can provide the basis for prewarning and intervention of danger and improve comfort performance during driving.

According to aforementioned works, it can be concluded that the intention identification of drivers is crucial to the driving safety of vehicles own and neighboring vehicles. In this paper, we establish the intention identification model with neural network trained by collected driving data. To make our model robust and precise, we combine the estimated intentions with trajectory prediction to figure out feasible and reasonable moving trace of vehicles for further collision probability evaluation.

B. Vehicular Position/Trajectory Prediction

Indeed, the reliable vehicular position and trajectory acquisition is a critical component of the cooperative driving technology in IoV. Lefèvre *et al.* [11] made a survey to classic motion prediction and risk assessment schemes for intelligent vehicles. They indicated that the motion prediction is one of the major challenges to detect dangerous situations and react accordingly in order to avoid or mitigate accidents. In their survey, they categorized the motion prediction approaches into physics-based, maneuver-based, and interaction-aware based on their degree of abstraction. The authors also highlighted the fact that the choice of a risk assessment method is tightly coupled with the choice of a motion prediction model. Ji *et al.* [12] proposed a path planning and tracking framework to maintain a collision-free path for autonomous vehicles. They first constructed a 3-D virtual dangerous potential field to generate a desired trajectory for collision avoidance when a vehicle collision with obstacles is likely to happen. After that, to track the planned trajectory for collision avoidance maneuvers, the path-tracking controller formulated the tracking task as a multiconstrained model predictive control problem and calculated the front steering angle to prevent the vehicle from colliding with a moving vehicle. Zhang *et al.* [13] proposed a vision-based UAV navigation model with obstacle detection and trajectory tracking. In their paper, the object detection and tracking are integrated into the dynamic Kalman filter model to figure out the feasible trajectory of UAV in the near future. In the detection phase, the object of interest is automatically detected and located by calculating the captured image

background; in the tracking phase, a dynamic Kalman filter is employed to provide a rough prediction to the object state in the near future.

From above investigations, it is worth noting that the researches on vehicular trajectory acquisition provides a good basis for the study of future collision probability. In this paper, the trajectories of vehicles are estimated with the Kalman filter model considering the steering angles of vehicles. In this way, different maneuvering cases can be taken into account at intersections, e.g., curve merge collision, blind point collision, and lane change collision.

C. Collision Probability/Risk Evaluation

With respect to the collision probability or risk evaluation, this research field is actually much mature and still attracting many studying efforts even today [14], [15]. Wang *et al.* [16] proposed a temporary-spatial collision warning model that gives the collision probability by calculating the time of the vehicle passing through the intersection. However, their works made a number of assumptions, e.g., constant speed, constant acceleration, thus leading to a more ideal result. Joerer *et al.* [17] presented a collision risk evaluation scheme by quantifying the probability of a future crash at intersections, depending on the situation in which a vehicle is receiving a beacon message. Their work demonstrated the importance of inter vehicle communication (IVC) in cooperative driving especially for safety related applications. On the contrary, although wireless communication could greatly increase the awareness range of vehicles, the randomness generated during IVC, such as channel fading, obstacle blocking, and packets collision, etc., make the IVC-based risk estimation not reliable in practice. Wu *et al.* [18] proposed a TTC-based intersection movement assist (IMA) model to reduce angle crashes at intersections. By a field operation test, the authors verified that the IMA has potential to reduce not only crash frequency but also crash severity.

Although studies on collision probability evaluation of vehicles are mature and popular, the solutions on how to assess the driving risks with drivers' intentions and vehicular trajectories considered, are still worth deep studying, especially for intersections, where complex conflicts between moving vehicles are readily occurring.

III. Proposed Framework

As mentioned above, urban intersections are known as a hotspot for traffic conflicts. In generally, the traffic conflict indicates the event that more than one vehicle is arriving at a specific zone simultaneously. In this way, if at least one of those cars takes non-normal traffic behaviors, e.g., wheel steering, speed changing, sudden parking, etc., a collision might occur unless the other vehicles take corresponding measures to avoid the possible collisions. For instance, as illustrated in Fig. 5, when vehicle A arrived at the intersection area, there is a probability that vehicle B may collide with A.

In this paper, for simplicity, we mainly study the typical two-way multilane intersection as depicted in Fig. 6, where vehicles can move toward different directions along each lane.

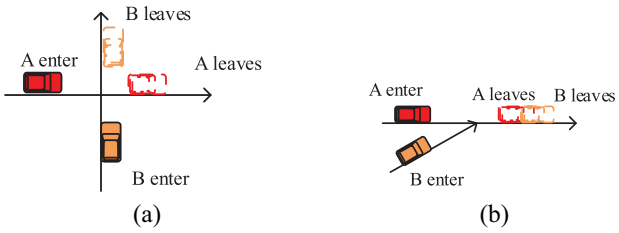

Fig. 5. Example of different intersection types. (a) X-intersection. (b) Y-intersection.

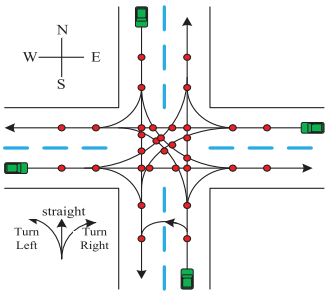

Fig. 6. Crossroads conflict points.

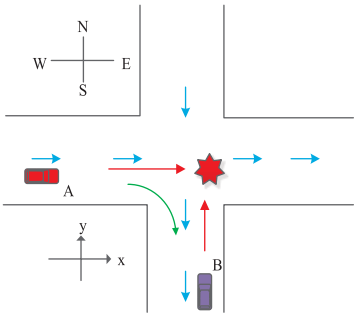

Fig. 7. One conflict scenario.

Generally, considering the great likelihood of vehicles for slow-down and/or steering at intersections, a collision may has high potential to occur especially at unsignalized intersections. In Fig. 6, the potential conflict points are marked as red dots. In general, it is verified that if the warning can be issued at least 2–3 s before the occurring of the conflicts, the driver may have chance to take reasonable actions to avoid the potential emergency [19]. In order to initiate the warnings timely and accurately, a risk evaluation process is necessary to quantify the probability of the potential collisions. If the collision probability in the next observation interval is high, then we can deem that the vehicle is in danger, and corresponding measures should be taken to handle the possible accidents; otherwise, if the collision probability is judged as low, it means that the vehicle is basically safe and can still keep the current driving state. In this paper, to establish the risk evaluation model and then provide quantified risk levels for the drivers or autonomous control units, the trajectories of vehicles are predicated as references. In practice, in addition to the vehicle's dynamics, e.g., speed, acceleration, position, the driver's intention has also significant impact on the resulted trajectory of a vehicle. Note that the driving intention is actually the

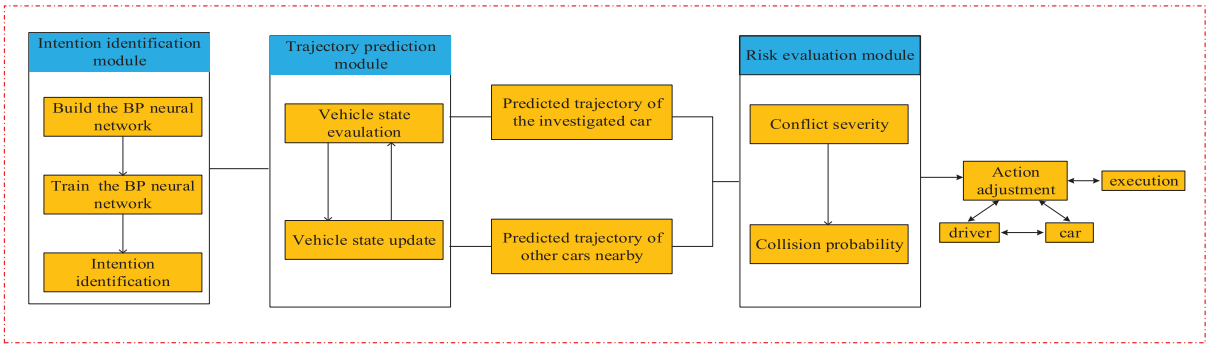

Fig. 8. Overall frame diagram.

internal psychological state of a driver formed during driving and associated with the present traffic and vehicular status, which can further determine the behavior of the driver in the near future. As shown in Fig. 7, given that the driver A's intention is to go straight, there is a potential conflict point between A and B. On the other hand, if the intentions of both A and B can be accurately identified beforehand, this conflict might be avoided by the proper actions taken by the drivers or the autonomous controls.

In light of the analysis above, the framework of our proposed risk evaluation model is illustrated in Fig. 8. In Fig. 8, the yellow modules are what we are concerned. At first, the investigated vehicle and its adjacent cars estimate their future positions and movement states with the help of the identified drivers' intentions. After that, with the help of wireless communication, the trajectories of all cars could be predicted and exchanged among vehicles by wireless communication. Next, through the predicted trajectories of these cars, the potential collision probability among them can be derived out. Finally, according to the obtained collision risk, the determination on whether to take appropriate actions to avoid possible collisions could be made. In summary, the framework can be mainly divided into three steps as follows.

1) The intention of a driver is modeled using the BP neural network.
2) The vehicle's trajectory is predicted by the Kalman filter model.
3) According to the trajectories of other vehicles' in the vicinity of intersections, the targeted vehicle can then evaluate the risk level, by which the next driving action is determined.

Next, we give out the detailed descriptions of each component of our framework in the following sections. For easy reference, the main notations used in this paper are summarized in Table I.

TABLE I
SUMMARY OF NOTATIONS

Notation	Description
I	the number of the neurons in the input layer
K	the number of the neurons in the output layer
V	the weight matrix of the input-hidden layer
W	the weight matrix of the hidden-output layer
v_{ji}	the general expression of V
w_{kj}	the general expression of W
α	the momentum coefficient
η	the learning rate
E	all the squared errors
δ_{yj}	the error signal from the hidden layer
δ_{ok}	the error signal from the output layer
d_k	the k^{th} neuron desired output value
o_k	the k^{th} neuron output value
$X(k)$	the vehicle state vector at time k
$x(k)$	the vehicles position in the x-axis
$y(k)$	the vehicles position in the y-axis
$v_x(k)$	the vehicles velocity in the x-axis
$v_y(k)$	the vehicles velocity in the y-axis
ψ_k	the rotation angle of the steering wheel
R_k	the circular arc radius
φ_k	the rotation angle of the front wheel
τ_k	the angle between the rear wheel and the x-axis
$\overrightarrow{a_k}$	the centripetal acceleration
$a_x(k)$	the acceleration in the x-axis
$a_y(k)$	the acceleration in the y-axis
T	the sampling interval
$W(k)$	the noise vector
$Q(k)$	the covariance matrix of the measurement noise
A	the state transition matrix
B	The control input matrix
$Z(k)$	The observation vector
$V(k)$	the observed noise vector
$R(k)$	the covariance matrix of observed noise
J	collision severity
$P(crash\|J)$	collision probability
$e_v(k+1)$	the relative speed error
$e_s(k+1)$	the relative distance error

IV. INTENTION IDENTIFICATION MODEL

The study in [8] suggested that people's wrong driving behavior is the major cause of road traffic accidents. In other words, because of the driver's erroneous driving operation, the vehicle may behave abnormally, thus leading to the possibility of accidents. Therefore, it is necessary to provide an intention speculating mechanism to identify the driver's intention as early as possible and accurately. Once obtaining the intentions of adjacent vehicles in advance, the targeted vehicle will have adequate time to adopt appropriate measures to avoid the potential risk. However, under the complex traffic environment, it is quite challenging to identify the driver's intention due to the time-varying operations. On the other side, the BP neural network is known as a kind of perception neural network, which has the ability of no-linear mapping, self-study, generalization, and fault-tolerant [20]. Thus, one promising approach for our issue

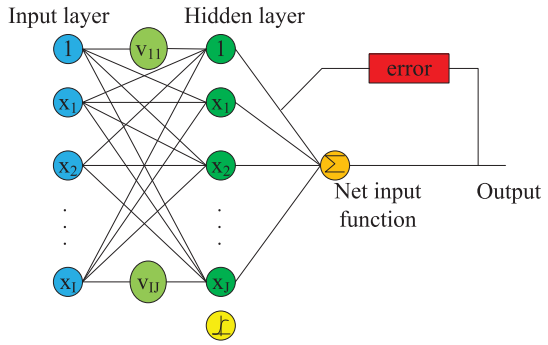

Fig. 9. Diagram of the regression based on BP neural network.

is to give the driving intention prediction using the logistic regression with BP neural network. A typical diagram of the regression scheme used in this paper is shown in Fig. 9. At first, each input parameter multiplied by the corresponding weight is input into the Net input function. Then, the obtained result from the Net input function is processed by the activation function. Finally, the error is feeded back to adjust the weights.

In this section, according to the regression method, we build the driving intention recognition model by fully taking into account different factors, such as the driver's action, the vehicle's state as well as the external environment. Next, we illustrate the detailed steps for building our model in the following sections.

A. Establish the Intention Identification Model

The BP neural network consists of input layer, hidden layer, and output layer. Each layer is composed of some neurons among which there is no connection. A full connection is formed between two adjacent layers. The information is transmitted from the input layer to the output layer through the hidden layer. In order to determine the neural network's structure, it is necessary to determine the following parameters, including the number of network layers, the number of input nodes, the number of output nodes, and the number of hidden layer nodes.

1) Network Layers: Generally, using the neural network to make the prediction and estimation, the more the network layers, the higher the network's accuracy is and the more the consumed time is. The existing researches have demonstrated that the three-layer network, where one hidden layer is sandwiched between one input layer and output layer, has the ability to simulate arbitrary nonlinear mapping if there are enough neurons in the hidden layer. Thus, considering the convergence rate and computation complexity, we adopt the three-layer neural network in this paper, as illustrated in Fig. 9.

2) Number of Input Nodes: In our proposed model, the number of input nodes is 4, i.e., the space headway, current steering angle, horizontal eye movement of the driver, and the lane change, respectively.

3) Number of Output Nodes: The output node in this paper is the steering angle only.

4) Number of Hidden Layer Nodes: The number of the neurons in the hidden layer depends on not only the number of the training samples and the regularity contained in these samples, but also the number of the neurons in the input layer and output layer. The best approach is to determine the number of the neurons in the hidden layer by sufficient trials. In order to determine the number of neurons in different layers, an empirical formula is used to provide the initial values, i.e., $m = \sqrt{I + K} + \vartheta$, where I is the number of the neurons in the input layer, K is the number of the neurons in the output layer, and ϑ is a constant selected within [1, 10].

Besides, in order to model the nonlinear prediction, the activation function is introduced in our proposed model. Considering the input range, the tanh function is used as the activation function.

B. Train the BP Neural Network

To speed up the process of finding a satisfactory solution, we adopt the generalized delta learning rule combining with the momentum method, as the weight-updating rule [21]. Next, we first give the theoretical background on learning the BP neural network and then present the process for training the network in detail.

1) Theoretical Background for Learning BP Neural Network: Denote net_j as the activation vector of the hidden layer j. Let

$$\mathbf{V} = \begin{bmatrix} v_{11} & v_{12} & \dots & v_{1J} \\ v_{21} & v_{22} & \dots & v_{2J} \\ \vdots & \vdots & \vdots & \vdots \\ v_{I1} & v_{I2} & \dots & v_{IJ} \end{bmatrix}$$

be the weight matrix of the input layer and $\mathbf{X} = [x_1 \quad x_2 \quad \dots \quad x_I]$ be the input vector, where I and J are the number of neurons in the input and hidden layer, respectively. Then, we have: $\text{net}_j = \mathbf{V} \cdot \mathbf{X}$.

A general expression of the weight adjustment of $\mathbf{V}$ is given by

$$\Delta v_{ji} = -\eta \frac{\partial E}{\partial v_{ji}},\ j \in \{1, 2, \dots, J\}, i \in \{1, 2, \dots, I\} \tag{1}$$

where η represents the learning rate which is set to 0.1 here, and E indicates all squared errors of the current training step.

Equation (1) can be further expressed as

$$\Delta v_{ji} = -\eta \frac{\partial E}{\partial \text{net}_j} \frac{\partial \text{net}_j}{\partial v_{ji}} = \eta \delta_{yj} x_i \tag{2}$$

where δ_{yj} represents the error signal from the hidden layer, and is denoted as

$$\delta_{yi} = -\eta \frac{\partial E}{\partial y_i} \frac{\partial y_i}{\partial \text{net}_j} = -\eta \frac{\partial E}{\partial y_i} f'(\text{net}_j). \tag{3}$$

Here, $(\partial E)/[(\partial y_j)] = (\partial)/[(\partial y_j)]\ ((1/2)\sum_{k=1}^{K} \{d_k - f[\text{net}_k(Y)]\}^2)$, where K is the number of the neurons and d_k is the desired value from the kth neuron in the output layer.

Based on (2) and (3), we have

$$\delta_{yj} = f_j^{'}(\text{net}_j)\sum_{k=1}^{K}\delta_{ok}w_{kj} \tag{4}$$

$$\Delta v_{ji} = \eta f_j^{'}(\text{net}_j)x_i\sum_{k=1}^{K}\delta_{ok}w_{kj} \tag{5}$$

where w_{kj} is the general expression of the hidden-output layer weight matrix $\mathbf{W}$, and δ_{ok} is the error signal from the output layer which can be written as: $\delta_{\text{ok}} = (d_k - o_k)(1-o_k)o_k$, where o_k is the kth neuron' s output value.

Similar to the error signal of the output layer, the error signal for the hidden layer can be also obtained as

$$\delta_{yj} = y_j(1-y_j)\sum_{k=1}^{K}\delta_{ok}w_{kj}. \tag{6}$$

The next step for the structure learning is to adjust w_{kj} and v_{ji} by using the following momentum method:

$$\Delta w_{kj}(t) = -\eta\delta_{ok}y_j + \alpha\Delta w_{kj}(t-1) \tag{7}$$

$$\Delta v_{ji}(t) = -\eta\delta_{yj}x_i + \alpha\Delta v_{ji}(t-1) \tag{8}$$

where α represents the momentum coefficient, which is randomly selected from [0, 1].

2) Training Process: We collect 1000 test data from 50 drivers by doing the double-lane change test on the driving simulators, the importance of which has significant increased in recent years, e.g., OT and VFP2 [22], [23]. Note that all the data are normalized. Then, the process to train our BP neural network is detailed steps as follows.

1) Input the training samples into the constructed BP neural network.
2) Set the upper limit of the training error $E_{\min} = \varepsilon$, where $0.01 \leq \varepsilon < 0.1$. The error boundary is determined according to the convergence speed and the learning accuracy of the neural network. When $E_{\min}$ is small, the learning performance can be increased at the cost of a slow convergence rate. If the $E_{\min}$ is large, the convergence speed will be accelerated but the learning performance is degraded.
3) Calculate the training error of the designed neural network.
4) Determine if the training error reaches the upper limit. If no, update the network weights. If yes, stop training.

V. Vehicular Trajectory Prediction

In this paper, to provide information exchange among different vehicles, the vehicle to infrastructure cooperative communication is applied to the unsignalized intersections, by which the vehicle traveling near the intersection can obtain the information of others nearby, e.g., position, speed, acceleration, and drivers' intentions. After that, we use the Kalman filter model to estimate the movement of each vehicle for the next observation interval.

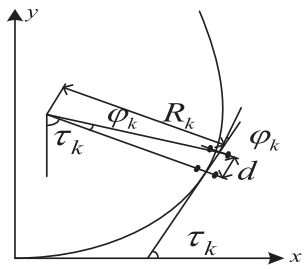

Fig. 10. Vehicle trajectory.

A. Vehicle Location Estimation

1) State Equation: Let $\mathbf{X}(k) = [x(k) \;\; y(k) \;\; v_x(k) \;\; v_y(k)]^T$, where k is the sequence number of the discreted intervals, $\mathbf{X}(k)$ represents the vehicle' state vector at the kth interval, $[x(k), y(k)]$ indicates the Cartesian coordinates at the kth interval, $v_x(k)$ and $v_y(k)$ denote the velocities in horizontal and vertical directions at the kth interval, respectively.

The system's state at the $(k+1)$th interval follows the following equation:

$$\mathbf{X}(k+1) = \mathbf{A}\mathbf{X}(k) + \mathbf{B}\mathbf{U}(k) + \mathbf{W}(k) \tag{9}$$

where $\mathbf{A}$ and $\mathbf{B}$ are the state transition matrix and control input matrix which apply the effect of the parameters at the kth interval on the system state at the $(k+1)$th interval, respectively. $\mathbf{W}(k)$ is the noise vector satisfying the normal distribution: $\mathbf{W}(k) \sim N(0, \mathbf{Q}(k))$, and $\mathbf{Q}(k)$ is the covariance matrix of the measurement noise.

As shown in Fig. 7, we divide the 2-D map into two orthogonal directions, where the position of x-axis and y-axis denotes the eastward and the north, respectively. According to the BP neural network proposed in Section IV, we can obtain the rotation angle of the steering wheel denoted by ψ_k. As shown in Fig. 10, the vehicle's short-term trajectory can be seen as a circular arc with the radius R_k.

Denote φ_k as the rotation angle of the front wheel. Then, we have: $\varphi_k = \beta \cdot \psi_k$, where β is a constant less than 1.

Letting d be the wheelbase, then R_k can be calculated as

$$R_k = \frac{d}{\tan\varphi_k} = \frac{d}{\tan(\beta\psi_k)}. \tag{10}$$

The angle between the rear wheel and the x-axis denoted by τ_k at the kth interval can be expressed as

$$\tau_k = \begin{cases} \varphi_0, & k = 0 \\ \varphi_k + \tau_{k-1}, & k \geq 1. \end{cases} \tag{11}$$

Based on (10), the centripetal acceleration $\overrightarrow{a_k}$ can be formulated as

$$\left|\overrightarrow{a_k}\right| = \frac{|V_k|^2}{R_k} = \frac{|V_k|^2}{d/\tan(\beta\psi_k)} \tag{12}$$

where $|V_k|$ is the speed.

By combining (11) and (12), the horizontal acceleration is derived as

$$a_x(k) = \left|\overrightarrow{a_k}\right|\sin\tau_k = \frac{|V_k|^2}{d/\tan(E\psi_k)}\sin\tau_k \tag{13}$$

and the vertical acceleration is given by

$$a_y(k) = \left|\overrightarrow{a_k}\right| \cos \tau_k = \frac{|V_k|^2}{d/\tan(E\psi_k)} \cos \tau_k. \tag{14}$$

We denote $\mathbf{U}(k)$ as $\begin{bmatrix} a_x(k) & a_y(k) \end{bmatrix}^T$ to reflect the impact of the steering wheel rotation angle on the accelerations in different directions.

The relationship between the throttle setting, vehicle's position, and velocity is described as follows:

$$x(k+1) = x(k) + v_x(k)T + \frac{a_x(k)T^2}{2} \tag{15}$$

$$y(k+1) = y(k) + v_y(k)T + \frac{a_y(k)T^2}{2} \tag{16}$$

$$v_x(k+1) = v_x(k) + a_x(k)T \tag{17}$$

$$v_y(k+1) = v_y(k) + a_y(k)T \tag{18}$$

where T is the sampling interval.

According to (9) and (15)–(18), we have

$$\mathbf{A} = \begin{bmatrix} 1 & 0 & T & 0 \\ 0 & 1 & 0 & T \\ 0 & 0 & 1 & 0 \\ 0 & 0 & 0 & 1 \end{bmatrix} \quad \mathbf{B} = \begin{bmatrix} \frac{T^2}{2} & 0 \\ 0 & \frac{T^2}{2} \\ T & 0 \\ 0 & T \end{bmatrix}.$$

2) Observation Equation: The real-time information related to the position, speed, and acceleration of vehicles can be easily obtained through sensors and exchanged among vehicles with wireless communications. Therefore, the observation vector $\mathbf{Z}(k)$ can be written as

$$\mathbf{Z}(k) = \mathbf{H}(k)\mathbf{X}(k) + \mathbf{V}(k) \tag{19}$$

where

$$\mathbf{H}(k) = \begin{bmatrix} 1 & 0 & 0 & 0 \\ 0 & 1 & 0 & 0 \\ 0 & 0 & 1 & 0 \\ 0 & 0 & 0 & 1 \end{bmatrix}$$

$\mathbf{V}(k)$ is the observed noise vector satisfying the normal distribution: $\mathbf{V}(k) \sim N(0, \mathbf{R}(k))$ and $\mathbf{R}(k)$ is the covariance matrix of observed noise at the kth interval.

B. Vehicle Location Update

In this section, the vehicle state's information can be updated as follows [24].

1) The one-step prediction equation can be expressed as

$$\hat{\mathbf{X}}(k|k-1) = \mathbf{A}\mathbf{X}(k-1|k-1) + \mathbf{B}\mathbf{U}(k-1) \tag{20}$$

where $\hat{\mathbf{X}}(k|k-1)$ indicates the estimated value at state k predicted with previous $k-1$ states.

2) The one-step prediction equation for covariance is

$$\mathbf{P}(k|k-1) = \mathbf{A}\mathbf{P}(k-1|k-1)A^T + \mathbf{Q}(k-1) \tag{21}$$

where $\mathbf{Q}(k-1)$ is the covariance matrix of the noise in state $k-1$.

3) The Kalman gain is

$$\mathbf{K}(k) = \mathbf{P}(k|k-1)\mathbf{H}^T(k)[\mathbf{H}(k)\mathbf{P}(k|k-1)\mathbf{H}^T(k) + R(k)]^{-1}. \tag{22}$$

4) Based on the predicted value $\hat{\mathbf{X}}(k|k-1)$ at state k, the optimal estimation $\hat{\mathbf{X}}(k|k)$ of the current state k is written as

$$\hat{\mathbf{X}}(k|k) = \hat{\mathbf{X}}(k|k-1) + \mathbf{K}(k)\Big[Z(k) - H(k)\hat{\mathbf{X}}(k|k-1)\Big]. \tag{23}$$

5) The error equation is

$$\mathbf{P}(k|k) = [\mathbf{I} - \mathbf{K}(k)\mathbf{H}(k)]\mathbf{P}(k|k-1) \tag{24}$$

where $\mathbf{P}(k|k-1)$ is the predicted covariance matrix of the state of vehicles, and $\mathbf{I}$ is the unit matrix.

After the system state equation and observation equation are established, it is necessary to initialize the state vector $\mathbf{X}(0|0)$, covariance $\mathbf{Q}$, $\mathbf{R}$ as well as the error covariance matrix $\mathbf{P}(0|0)$.

1) The initial state vector $\mathbf{X}(0|0)$ can be estimated based on the actual state. Since the Kalman filter considers the subsequent measurement vectors comprehensively, the influence of the initial estimation error is regarded as trivial.
2) The parameters in covariance $\mathbf{Q}$ depend on the accuracy of the system state equation. Generally, it is difficult to set these arguments accurately. Therefore, these parameters can be determined after several experiments and simulations, and the arguments will be adjusted until the optimal results are reached.

Based on the algorithm, the future trajectories of vehicles could be estimated.

VI. Collision Probability Estimation

In order to estimate the severity of vehicle collision, two major collision indexes, namely, the TTC and PET [25], [26] are often adopted by the existing work. Different from the previous work, in this section, we first give the scenarios, where there are potential conflicts and then present a metric named "collision probability" to provide the guidance for determining the future actions.

A. Potential Conflict Scenarios

Consider the two-way multilane intersection as illustrated in Fig. 6, where vehicles can move toward different directions along each road segment. Without loss of generality, we take vehicle A for example to give the potential conflict scenarios in this section, as shown in Fig. 11. Fig. 11(a)–(e) indicate the scenarios, where when A goes straight, there is a chance that A collides with B, and Fig. 11(f)–(i) represent the cases that when A makes a turn, there is a conflict probability. When one vehicle finds that it is faced with one of these scenarios listed in Fig. 11, it should make the risk evaluation to judge whether it is in danger. In this way, the vehicle can take proper measures to deal with the potential risk in advance.

B. Collision Probability

Actually, the collision severity is not only related to the intervehicle distance, but also to the speeds of collided vehicles. Therefore, we improve the traditional algorithms that only

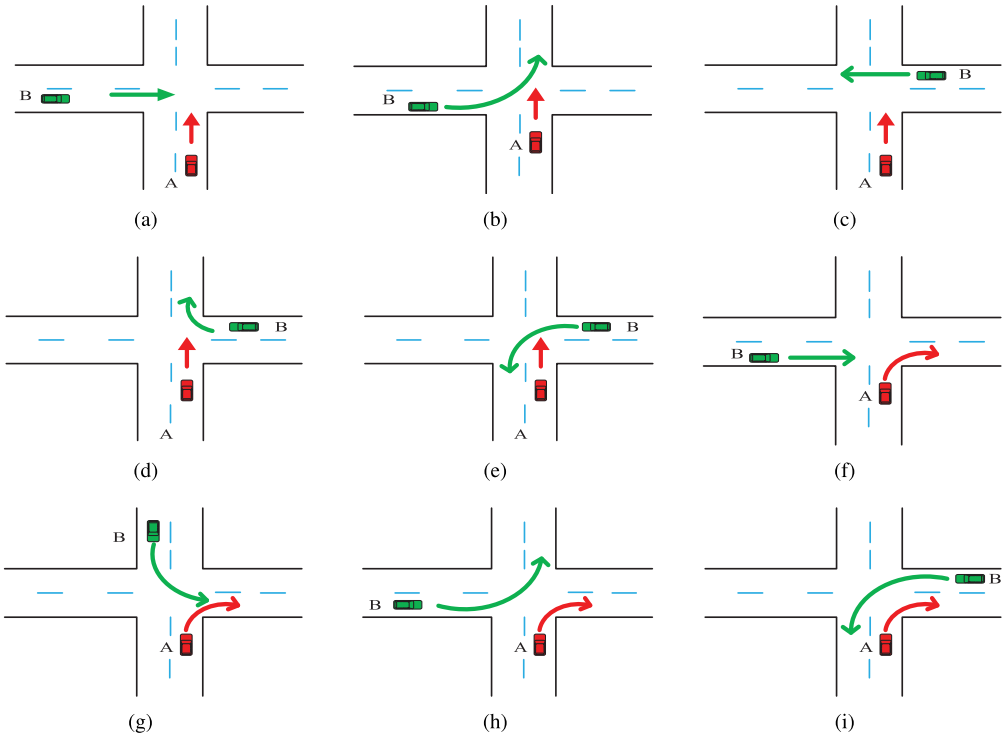

Fig. 11. Different potential conflict scenarios.

rely on the intervehicle distance $\Delta s(k)$ to determine the conflict level by introducing the speed difference Δv. In this way, the severity level J at time k between vehicle A and B can be given by

$$J = \frac{\Delta s(k)}{\Delta v(k)} = \frac{\sqrt{(x_a(k) - x_b(k))^2 + (y_a(k) - y_b(k))^2}}{\sqrt{(v_{ax}(k) - v_{bx}(k))^2 + \left(v_{ay}(k) - v_{by}(k)\right)^2}} \tag{25}$$

where $(x_a(k), y_a(k))$ and $(x_b(k), y_b(k))$ are their coordination positions, respectively, and $(v_{ax}(k), v_{ay}(k))$, $(v_{bx}(k), v_{by}(k))$ are their velocity vectors, respectively. A decreasing exponential function is introduced to describe the collision probability, i.e.,

$$y = a + b \times \exp\left(-\frac{z}{c}\right), \quad a, b, c \text{ is constant.} \tag{26}$$

The collision probability y is between [0, 1]. Let $a = 0$ and $b = 1$. The coefficient c can reflect the degree of curve bending. Given J, the collision probability denoted by $P(\text{crash}|J)$ can be expressed as

$$P(\text{crash}|J) = \exp\left(-\frac{1}{c} \cdot J\right). \tag{27}$$

Finally, according to the collision probability, the driver can determine whether to take some measures to avoid the potential collision accidents.

VII. Numercial Results and Performance Evaluation

In this section, we conduct an extensive simulation to evaluate the performance of our proposed model. Some assumptions are presented to facilitate the test of our models: each vehicle is equipped with sensors, such as speed and brake pressure and has a wireless transceiver, e.g., dedicated short range communications; the GPS equipment is used to get the location and speed information; the intelligent driver model (IDM) is used in this paper to model the moving behavior of vehicles on a road.

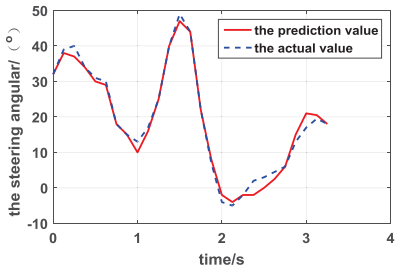

Fig. 12. Comparison between the prediction value and the actual one.

A. Evaluation of BP Neural Network Model

We collect 1000 test data from 50 drivers by doing the double-lane change test on the driving simulators to do the crossing validation. Note that all the data are normalized. With the assistance of MATLAB toolbox in artificial neural networks, our proposed model is trained to get the actual net among different neurons.

Fig. 12 shows the comparison results between the predicted value from the BP neural network and the actual value. From this result, it can be found that the predicted value of the steering angle agrees well with the actual experimental value. This demonstrates the accuracy of our proposed model.

TABLE II
KINEMATIC VARIABLES AND COLLISION PROBABILITY FOR CASE ONE

Subject	Vehicle A				Vehicle B				J
	x_1/m	y_1/m	$v_{x_1}(m/s)$	$v_{y_1}(m/s)$	x_2/m	y_2/m	$v_{x_2}(m/s)$	$v_{y_2}(m/s)$	
1	5.06	-20.51	0.00	10.10	-20.12	-5.07	10.20	-0.01	0.0822
2	5.06	-17.32	-0.02	10.20	-17.51	-5.10	10.11	0.02	0.1092
3	5.03	-14.21	0.00	10.11	-14.54	-5.05	10.02	0.00	0.1452
4	5.03	-11.71	0.04	10.01	-11.90	-5.06	10.13	-0.04	0.1871
5	5.11	-8.60	0.00	9.90	-8.22	-5.15	10.00	0.01	0.2567
6	5.11	-5.21	-0.02	10.00	-5.33	-5.13	9.92	0.04	0.3527
7	5.08	-2.42	0.00	10.11	-2.62	-5.06	10.02	0.00	0.4708
8	5.08	1.30	-0.04	10.02	1.50	-5.07	10.10	0.00	0
9	5.01	4.71	-0.05	10.12	4.32	-5.03	10.21	0.03	0
10	5.01	7.20	-	-	7.51	-5.03	-	0	-

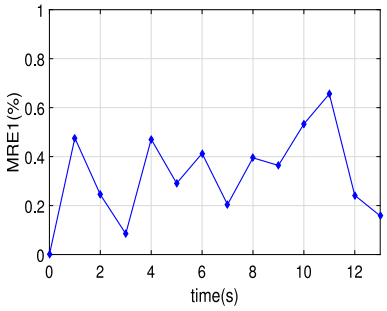

Fig. 13. Vehicle speed error.

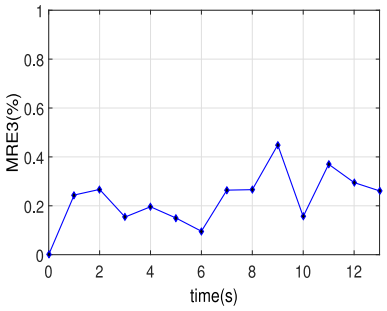

Fig. 14. Vehicle position error.

B. Evaluation of Kalman Filter Model

In order to verify the accuracy of the prediction model, we perform the experiments based on the generated mobility trace using IDM. In addition, the mean relative error is used to further demonstrate the efficiency of the proposed Kalman filter model.

The following metrics are used to verify the performance of our proposed Kalman filter model in terms of the vehicular dynamic prediction:

$$e_v(k+1) = \left| \frac{v(k+1) - v(k+1|k)}{v(k+1)} \right| \tag{28}$$

$$e_s(k+1) = \left| \frac{s(k+1) - s(k+1|k)}{s(k+1)} \right| \tag{29}$$

where $e_v(k+1)$ and $e_s(k+1)$ represent the relative errors of the speed and the intervehicle distance in the $(k+1)$th interval, respectively.

With N test results, the MRE can be given by

$$\text{MRE} = \frac{\sum_k e_v(k+1)}{N} \tag{30}$$

$$\text{MRE} = \frac{\sum_k e_s(k+1)}{N}. \tag{31}$$

Figs. 13 and 14 show the MRE of the vehicle speed and position, respectively. From Figs. 13 and 14, it can be found that the maximum relative error is no more than 0.7%, demonstrating the accuracy of our state prediction model.

C. Evaluation of Risk Evaluation Model

1) Simulation Settings: We simulate a typical two-way multilane intersection with size 21 m × 21 m. For convenience, we establish the coordinate system as shown in Fig. 7 with the center of the intersection as the origin. In this section, we mainly consider three potential scenarios to analyze the collision probability using our proposed model as illustrated in Fig. 15. The parameters needed and kinematic variables are listed in Tables II–IV, respectively. For each case, we extract ten frames, which cover the time span from the moment each vehicle is intended to cross the intersection to the instant it leaves the intersection.

2) Simulation Results and Analysis: Fig. 16 shows the collision probability with the time varying corresponding to the case one illustrated in Fig. 15(a). From the figure, it can be found that in the beginning, the collision probability is increased with the increase of the frame number, and after a period of time, the collision probability is rapidly reduced. This is reasonable. In case one, both of vehicles A and B are intended to go straight. At first, A is located in $(5.06, -20.5)$ and B is located in $(-20.1, -5.07)$. They are moving along the ways the arrows lead, respectively. As time varies, A and B are approaching the intersection. In this situation, the geographic intervehicle distance separating them with each other is decreasing. At the seventh frame, the distance between them achieves a lesser value. Based on the concept of conflict severity, it is known that the relative distance is proportional to the conflict severity, which means that the less the distance, the larger the collision probability. Thus, the collision probability is maximized at the time. However, from the eighth frame, the collision probability drops sharply. This is because that at that moment, both of A and B have crossed the intersection. Thus, there is no conflict risk between them.

Fig. 17 describes the collision probability as one function of the frame number corresponding to the case two illustrated in Fig. 15(b). In this case, A has the intention to make one

TABLE III
KINEMATIC VARIABLES AND COLLISION PROBABILITY FOR CASE TWO

Subject	Vehicle A				Vehicle B				J
	x_1/m	y_1/m	$v_{x_1}(m/s)$	$v_{y_1}(m/s)$	x_2/m	y_2/m	$v_{x_2}(m/s)$	$v_{y_2}(m/s)$	
1	-20.00	-5.00	10.33	0.20	-5.01	20.01	0.00	10.00	0.1351
2	-16.9	-4.92	10.27	0.23	-5.01	17.02	-0.01	9.93	0.1790
3	-13.82	-4.85	9.90	0.03	-5.03	14.20	0.00	10.03	0.2284
4	-10.85	-4.84	9.20	-0.37	-5.03	11.00	0.01	9.98	0.2815
5	-8.09	-4.95	4.43	-1.93	-5.01	8.02	0.01	9.98	0.2354
6	-6.76	-5.53	2.13	-5.3	-5.06	5.04	-0.02	10.01	0.1265
7	-6.16	-7.12	0.37	-5.93	-5.04	2.00	0.01	9.94	0.1054
8	-6.01	-8.90	0.33	-11.73	-5.02	-1.20	0.01	10.00	0.0101
9	-6.00	-12.42	0.00	-10.10	-5.00	-4.20	0.01	10.02	0.0001
10	-6.00	-15.45	-	-	-5.04	-7.23	0.03	0	-

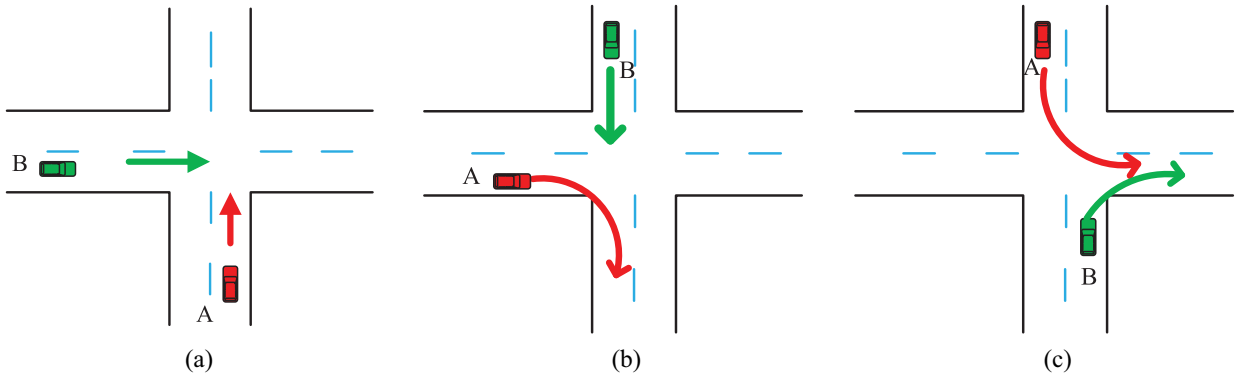

Fig. 15. Simulation scenarios. (a) Case one: straight-straight. (b) Case two: straight-turn. (c) Case three: turn-turn.

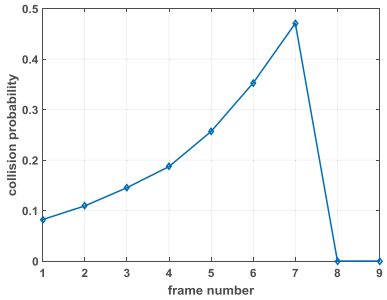

Fig. 16. Collision probability for case one.

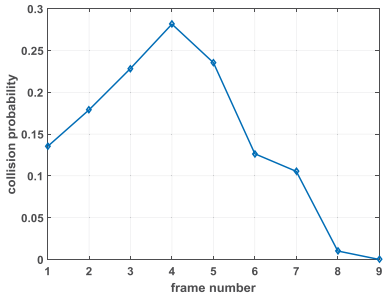

Fig. 17. Collision probability for case two.

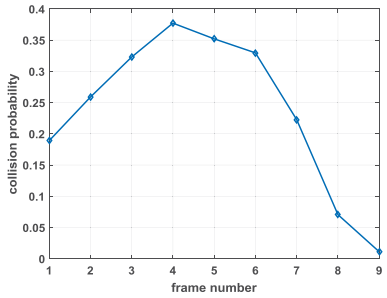

Fig. 18. Collision probability for case three.

turn, while B is intended to keep going straight. Considering the their further trajectories, there is a chance that they collide with each other because of the overlap of their positions. From the figure, it is noticed that similar with Fig. 16, the collision probability is increased at first, but reduced at last. From the first frame to the fourth frame, B is going straight and A will conduct the turning behavior. During the process, they are approaching the intersection, thus decreasing the intervehicle distance. At the fourth frame, the collision probability reaches the maximum due to the large reduction in the distance. After the moment, with the time varying, due to the impact of the intervehicle distance and the relative speed, the collision probability is reduced.

Fig. 18 illustrates the collision probability of two vehicles with time varying corresponding to case three illustrated in Fig. 15(c). In the beginning, the intervehicle distance between A and B is larger, thus exhibiting the lower collision probability. With the time changing, A and B are starting turn. Then, they are approaching each other. From this figure, it is noticed that from the first frame to the fourth frame, two vehicles are approaching the conflict point. During this process, conflict severity becomes more and more small and the collision probability is increasing. At the fourth frame, conflict severity achieves its minimum value and the collision probability is maximized greater, indicating that there is a conflict

TABLE IV
KINEMATIC VARIABLES AND COLLISION PROBABILITY FOR CASE THREE

Subject	Vehicle A				Vehicle B				J
	x_1/m	y_1/m	$v_{x_1}(m/s)$	$v_{y_1}(m/s)$	x_2/m	y_2/m	$v_{x_2}(m/s)$	$v_{y_2}(m/s)$	
1	-5.00	20.00	0.01	-13.67	5.00	-20.00	0.27	10.33	0.1794
2	-4.98	15.90	0.20	-14.00	5.80	-16.90	0.23	10.27	0.2432
3	-4.92	11.71	0.67	-12.67	5.15	-13.82	0.03	9.90	0.2966
4	-4.72	7.90	0.73	-10.00	5.16	-10.85	-0.37	9.20	0.3322
5	-4.50	4.90	3.67	-8.00	5.05	-8.09	4.30	4.43	0.2739
6	-3.40	2.51	6.00	-6.33	6.34	-6.76	6.47	2.00	0.1998
7	-1.60	0.60	9.67	-4.00	8.28	-6.16	9.73	0.50	0.0699
8	1.30	-0.61	9.83	-2.00	11.20	-6.01	10.00	0.03	0.0040
9	4.25	-1.20	11.83	-0.67	14.20	-6.00	12.67	0.00	0.0001
10	7.80	-1.41	-	-	18.00	-6.00	-	-	-

risk. After fourth frame, two vehicles are leaving the conflict point and the collision probability is becoming smaller.

VIII. CONCLUSION

In this paper, a cooperative driving scheme is proposed among vehicles around intersections. At first, we use the BP neural network to model the driver's intention and output the angle of the steering wheel corresponding to the identified driver's intention. Then, the obtained steering angle is input as the control matrix of the Kalman filter model, by which the trajectory of each vehicle is predicted. Finally, the collision probability model at the intersection is given according to the conflict determination based on predicted trajectories of vehicles. Numerical results show that our model has a high precision in terms of risk recognition.

A. Limitations

It is worth noting that we did not make comparisons among different schemes with respect to driving risk evaluations. Actually, we have reviewed many references to find similar works with ours for further performance comparisons. However, there was no work exactly to combine the driver's intention identification, trajectory prediction, and collision probability estimation together. Therefore, we demonstrate the accuracy of our model by comparing the simulation results with collected dataset on a practical driving simulator. In addition, the identified driver's intention is transformed to the angle of the steering wheel through a neural network, which is actually a simplification to the complex driving behaviors and vehicular dynamics. At last, our proposed collision evaluation model is just applicable to the intersections, where vehicles are usually driving slowly. In this way, the conflict between trajectories can be readily equivalent to the region overlap problem. However, in practice, the trajectory conflict is time-dependent. In other words, only the conflict of trajectories precisely on the same occasion can be realized as a potential collision.

B. Future Work

Our future work will investigate more complex collision cases under practical transportation scenarios. In addition, the deep learning skill will be introduced to generate more accurate model for driving risk evaluations.

REFERENCES

[1] K. Zheng, Q. Zheng, P. Chatzimisios, W. Xiang, and Y. Zhou, "Heterogeneous vehicular networking: A survey on architecture, challenges, and solutions," *IEEE Commun. Surveys Tuts.*, vol. 17, no. 4, pp. 2377–2396, 4th Quart., 2017.

[2] O. Kaiwartya *et al.*, "Internet of vehicles: Motivation, layered architecture, network model, challenges, and future aspects," *IEEE Access*, vol. 4, pp. 5356–5373, 2016.

[3] L.-W. Chen and P.-C. Chou, "BIG-CCA: Beacon-less, infrastructureless, and GPS-less cooperative collision avoidance based on vehicular sensor networks," *IEEE Trans. Syst., Man, Cybern., Syst.*, vol. 46, no. 11, pp. 1518–1528, Nov. 2016.

[4] C. Chen *et al.*, "A congestion avoidance game for information exchange on intersections in heterogeneous vehicular networks," *J. Netw. Comput. Appl.*, vol. 85, pp. 116–126, May 2017.

[5] C. Chen, X. Liu, T. Qiu, L. Liu, and A. K. Sangaiah, "Latency estimation based on traffic density for video streaming in the Internet of Vehicles," *Comput. Commun.*, vol. 111, pp. 176–186, Oct. 2017.

[6] M. Aswad, S. Al-Sultan, and H. Zedan, "Context aware accidents prediction and prevention system for VANET," in *Proc. 3rd Int. Conf. Context Aware Syst. Appl.*, 2014, pp. 162–168.

[7] W. Woerndl, M. Brocco, and R. Eigner, "Context-aware recommender systems in mobile scenarios," *Int. J. Inf. Technol. Web Eng.*, vol. 4, no. 1, pp. 67–85, 2009.

[8] N. A. Stanton and P. M. Salmon, "Human error taxonomies applied to driving: A generic driver error taxonomy and its implications for intelligent transport systems," *Safety Sci.*, vol. 47, no. 2, pp. 227–237, 2009.

[9] M. N. Husen and S. Lee, "Continuous car driving intention recognition with syntactic pattern approach," in *Proc. IEEE Int. Conf. Inf. Commun. Technol.*, Kuala Lumpur, Malaysia, 2016, pp. 71–76.

[10] L. He, C.-F. Zong, and C. Wang, "Driving intention recognition and behaviour prediction based on a double-layer hidden Markov model," *J. Zhejiang Univ. Sci. C*, vol. 13, no. 3, pp. 208–217, 2012.

[11] S. Lefèvre, D. Vasquez, and C. Laugier, "A survey on motion prediction and risk assessment for intelligent vehicles," *ROBOMECH J.*, vol. 1, no. 1, pp. 1–14, Jul. 2014.

[12] J. Ji, A. Khajepour, W. W. Melek, and Y. Huang, "Path planning and tracking for vehicle collision avoidance based on model predictive control with multiconstraints," *IEEE Trans. Veh. Technol.*, vol. 66, no. 2, pp. 952–964, Feb. 2017.

[13] J. Zhang, W. Liu, and Y. Wu, "Novel technique for vision-based UAV navigation," *IEEE Trans. Aerosp. Electron. Syst.*, vol. 47, no. 4, pp. 2731–2741, Oct. 2011.

[14] C. Chen *et al.*, "A rear-end collision prediction scheme based on deep learning in the Internet of Vehicles," *J. Parallel Distrib. Comput.*, Aug. 2017, doi: 10.1016/j.jpdc.2017.08.014.

[15] C. Chen, M. Li, J. Sui, K. Wei, and Q. Pei, "A genetic algorithm-optimized fuzzy logic controller to avoid rear-end collisions," *J. Adv. Transp.*, vol. 50, no. 8, pp. 1735–1753, 2016.

[16] J. Wang, X. Xue, R. Chai, and N. Cao, "A temporal-spatial collision warning method at non-signalized intersection," *Procedia Eng.*, vol. 137, no. 2016, pp. 827–835, 2016.

[17] S. Joerer *et al.*, "A vehicular networking perspective on estimating vehicle collision probability at intersections," *IEEE Trans. Veh. Technol.*, vol. 63, no. 4, pp. 1802–1812, May 2014.

[18] K.-F. Wu, N. Ardiansyah, and W.-J. Ye, "An evaluation scheme for assessing the effectiveness of intersection movement assist (IMA) on improving traffic safety," *Traffic Injury Prevent.*, Oct. 2017, pp. 1–5, doi: 10.1080/15389588.2017.1363891.
[19] M. Liebner and F. Klanner, *Driver Intent Inference and Risk Assessment*. Cham, Switzerland: Springer Int., 2016.
[20] K. Hamad, M. A. Khalil, and A. Shanableh, "Modeling roadway traffic noise in a hot climate using artificial neural networks," *Transp. Res. D, Transp. Environ.*, vol. 53, pp. 161–177, Jun. 2017.
[21] D. Lee and H. Yeo, "Real-time rear-end collision-warning system using a multilayer perceptron neural network," *IEEE Trans. Intell. Transp. Syst.*, vol. 17, no. 11, pp. 3087–3097, Nov. 2016.
[22] L. Meuleners and M. Fraser, "A validation study of driving errors using a driving simulator," *Transp. Res. F, Traffic Psychol. Behav.*, vol. 29, pp. 14–21, Feb. 2015.
[23] E. Baumgartner, A. Ronellenfitsch, H.-C. Reuss, and D. Schramm, "Using a dynamic driving simulator for perception-based powertrain development," *Transp. Res. F, Traffic Psychol. Behav.*, Oct. 2017, doi: 10.1016/j.trf.2017.08.012.
[24] T. Schuhmann, W. Hofmann, and R. Werner, "Improving operational performance of active magnetic bearings using Kalman filter and state feedback control," *IEEE Trans. Ind. Electron.*, vol. 59, no. 2, pp. 821–829, Feb. 2012.
[25] J. Hillenbrand, A. M. Spieker, and K. Kroschel, "A multilevel collision mitigation approach—Its situation assessment, decision making, and performance tradeoffs," *IEEE Trans. Intell. Transportation Syst.*, vol. 7, no. 4, pp. 528–540, Dec. 2006.
[26] N. Nadimi, H. Behbahani, and H. Shahbazi, "Calibration and validation of a new time-based surrogate safety measure using fuzzy inference system," *J. Traffic Transp. Eng.*, vol. 3, no. 1, pp. 51–58, 2016.

Chen Chen (M'09) received the B.Eng., M.Sc., and Ph.D. degrees in electrical engineering and computer science (EECS) from Xidian University, Xi'an, China, in 2000, 2006, and 2008, respectively.

He is currently an Associate Professor with the Department of EECS, Xidian University, where he is the Associate Director of the Intelligent Transportation Research Laboratory. He is also the Director of the Engineering Technology Transfer Center, Xi'an, in edge computing. He was a Visiting Professor with the Department of Electrical Engineering and Computer Science, University of Tennessee, Knoxville, TN, USA, from 2013 to 2014. He has authored or co-authored 2 books and over 70 scientific papers in international journals and conference proceedings. He has contributed to the development of 2 copyrighted software systems and invented 40 patents.

Dr. Chen serves as the General Chair, the PC Chair, the Workshop Chair or a TPC member for numerous conferences. He is a Senior Member of the China Computer Federation and a member of the ACM and the Chinese Institute of Electronics.

Lei Liu received the B.Eng. degree in communication engineering from Zhengzhou University, Zhengzhou, China, in 2010, and M.Sc. degree in communication engineering from Xidian University, Xi'an, China, in 2013, where he is currently pursuing the Ph.D. degree.

His current research interests include intelligent transportation and the Internet of Things.

Tie Qiu (M'12–SM'16) received the M.Sc. and Ph.D. degrees in computer science from the Dalian University of Technology, Dalian, China, in 2005 and 2012, respectively.

He is currently a Full Professor with Tianjin University, Tianjin, China. He was a Visiting Professor with the Department of Electrical and Computer Engineering, Iowa State University, Ames, IA, USA, from 2014 to 2015. He has contributed to the development of 4 copyrighted software systems and holds 15 patents.

Dr. Qiu serves as an Associate Editor of IEEE ACCESS, *Computers and Electrical Engineering* (Elsevier), and *Human-Centric Computing and Information Sciences* (Springer). He is an Editorial Board member of *Ad Hoc Networks* (Elsevier) and the *International Journal on AdHoc Networking Systems* and has been a Guest Editor of *Future Generation Computer Systems* (Elsevier). He serves as the General Chair, the PC Chair, the Workshop Chair, the Publicity Chair, the Publication Chair, or a TPC member of numerous conferences. He has authored/co-authored 8 books and over 100 scientific papers in international journals and conference proceedings such as ToN, TMC, TII, TIP, IEEE TRANSACTIONS ON COMMUNICATIONS, IEEE SYSTEMS JOURNAL, the IEEE INTERNET OF THINGS JOURNAL, and *Computer Networks*. He is a Senior Member of the China Computer Federation and a Senior Member of the ACM.

Zhiyuan Ren (M'09) received the M.S. and Ph.D. degrees in communication and information system from Xidian University, Xi'an, China, in 2007 and 2011, respectively.

He is an Associate Professor with the School of Telecommunication Engineering, Xidian University. He has authored of co-authored over ten journals and conference publications. His current research interests include distributed computing, mobile edge computing, and network virtualization in the industry Internet of Things environment.

Jinna Hu received the B.Eng. degree in information security from Xidian University, Xi'an, China, in 2015, where she is currently pursuing the Ph.D. degree at the State Key Laboratory of Integrated Services Networks.

Her current research interests include vehicular ad-hoc networks, wireless communication, and game theory.

Fang Ti received the B.Eng. degree in electronic information science and technology from Qufu Normal University, Rizhao, China, in 2014. She is currently pursuing the master's degree at the State Key Laboratory of Integrated Services Networks, Xidian University, Xi'an, China.

Her current research interests include vehicular ad-hoc networks, wireless communication, and time sensitive networking.